Title
Assessment of orchard N losses to groundwater with a vadose zone monitoring network

Journal
Agricultural Water Management, 172(C)

ISSN
0378-3774

Authors
Baram, S
Couvreur, V
Harter, T
et al.

Publication Date
2016-07-01

DOI
10.1016/j.agwat.2016.04.012

Peer reviewed

Agricultural Water Management 172 (2016) 83–95

Contents lists available at ScienceDirect

Agricultural Water Management

journal homepage: www.elsevier.com/locate/agwat

Assessment of orchard N losses to groundwater with a vadose zone monitoring network

S. Baram[a,*], V. Couvreur[a], T. Harter[a], M. Read[b], P.H. Brown[c], J.W. Hopmans[a], D.R. Smart[b]

[a] Department of Land, Air & Water Resources, University of California Davis, One Shields Avenue, Davis, CA 95616, United States
[b] Department of Viticulture and Enology, University of California Davis, One Shields Avenue, Davis, CA 95616, United States
[c] Department of Plant Sciences, University of California Davis, One Shields Avenue, Davis, CA 95616, United States

ARTICLE INFO

Article history:
Received 2 February 2016
Received in revised form 13 April 2016
Accepted 18 April 2016

Keywords:
Nitrate
Best-management-practice
Leaching
Fertigation
Flooding

ABSTRACT

A 2-year study was conducted to explore the impact of current and alternative best management practices (BMPs) of irrigation and fertigation on nitrate (NO_3^-) leaching below the root zone. Using a fully randomized complete block design, three fertigation strategies were compared: current BMP with and without accounting for NO_3^--N in irrigation-water, and a high frequency fertigation treatment with low-N concentration applications. Temporal changes in water content, pore water NO_3^- concentrations and soil water potential were monitored within and below the root zone to a soil depth of 3 m at eight sites in an almond and a pistachio orchard. NO_3^- concentrations below the root zone ranged from <1 mg L^{-1} to more than 2400 mg L^{-1} (almond), and up to 11,000 (pistachio) mg L^{-1}, with mean concentrations of 326 and 4631 mg L^{-1}, respectively. Within the fertigation cycle, fertilizer injection at the end of an irrigation event generally resulted in lower NO_3^- losses below the root zone compared with fertilizer injection mid-way through the irrigation. Pre-bloom and post-harvest flood irrigation in the almond orchard caused deep soil wetting and flushing of NO_3^- below the root zone, threatening groundwater quality. Statistical analysis using principal component analysis, Chi-squared Automatic Interaction Detector and the Artificial Neural Network showed that most of the deep soil NO_3^- concentration variability could not be explained by irrigation duration, fertigation timing or local variations in soil physical characteristics. However, mass balance estimates for water and N indicated the annual orchard average N loss could be estimated based on eight monitoring sites in spite of the inherent spatial variations in soil properties and the spatiotemporal variations in water and NO_3^- applications. The study indicated that reduction of N losses at the orchard scale would require alternative fertigation and irrigation practices, including better control of fertigation amounts and irrigation duration.

1. Introduction

Nitrate (NO_3^-) continues to be a major source of nonpoint-source pollution in agricultural ecosystems. Elevated NO_3^- concentrations in groundwater are frequently associated with leaching from irrigated land, especially in agricultural groundwater basins where leaching is a major component of recharge to local groundwater (Böhlke 2002; Green et al., 2008; Botros et al., 2012; Viers et al., 2012). Nitrogen budgeting has long been used as a site and crop specific tool to maximize yields, while minimizing fertilizer use. But best nutrient management practices (BMPs) generally are neither designed nor tested explicitly for preventing groundwater contamination by NO_3^-. BMPs are based on field, plot, and laboratory studies of N-cycling in the root zone (e.g., Allaire-Leung et al., 2001). Knowledge of spatial and temporal variability in NO_3^- concentrations below the root zone at the field scale (potential leachable NO_3^-) from such studies is exceedingly limited but essential to assess the long-term effectiveness of N-fertilizer BMPs with respect to groundwater protection, using vadose zone field instrumentation.

Our current understanding of NO_3^- distribution, fate, and transport below the root zone at the field or orchard scale (>0.10 km^2) is limited by typically prohibitive experimental costs to address the large degree of spatial variability (Onsoy et al., 2005; Botros et al., 2012). At the orchard scale, spatial variability in NO_3^- concentrations is mainly driven by the inherent spatial variability of soil physical-chemical properties, but also by the spatio-temporal variability of water and fertilizer applications. These factors contribute

* Corresponding author at: 116 Veimeyer Hall, University of California Davis, 95616, United States.
E-mail address: sbaram@ucdavis.edu (S. Baram).

http://dx.doi.org/10.1016/j.agwat.2016.04.012
0378-3774/

to highly nonuniform NO_3^- distribution observed in the subsurface (Onsoy et al., 2005; Mohannty and Kanwar 1994). A considerable amount of research has been done to study the N-mass balance in the root zone (e.g., Stenger et al., 2002; Ilsemann et al., 2001). But to gain better understanding of orchard N-losses to groundwater, especially in regions with thick unsaturated zones (>10 m) and potentially long travel times due to low recharge rates, a need exists to monitor losses immediately below the effective root zone (usually below a depth of 1.5 m), rather than in groundwater monitoring wells. Deep vadose zone studies have used intensive core sampling (Onsoy et al., 2005; Botros et al., 2012) or 3-D numerical modeling (Russo et al., 2014, 2013) to study the flow and transport of NO_3^- below irrigated orchards. In these studies, field sampling, mass balance approaches and multi-dimensional flow and transport simulations highlight the large degree of spatio-temporal variability of the NO_3^- losses to below the root zone, demonstrating the challenges to accurately estimate field scale leaching losses from deep soil samples. Results suggest that a large fraction of the soil water was immobile, while a smaller mobile water fraction was responsible for NO_3^- transport.

Since the year 2000, almond and pistachio orchards have doubled in acreage to over half a million hectare (CDFA, 2014) in California. Driven in part by pollution prevention efforts, but also to increase yields, nitrogen (N) management in almonds has been the subject of much research (Lopus et al., 2010; Micke, 1996). Current BMPs are based on a mass balance approach, where the seasonal applied N-loads account for yield-estimates and vegetative growth while assuming 70% N uptake efficiency (Silva et al., 2013; Siddiqui and Brown, 2013). These BMPs take into account pumped groundwater (well water) NO_3^--N, as equivalent to synthetic fertilizer at a direct one-to-one ratio. This utilization of groundwater NO_3^--N in the annual N-budget is defined herein as Pump and Fertilize (P&F). The P&F approach has the potential to reduce N-losses to the environment, while providing a means for mitigating groundwater contaminated by NO_3^- (King et al., 2012).

To date, BMPs guidelines do not provide recommendations regarding the timing of fertilizer injections within the irrigation cycle of a fertigation event (beginning/middle/end of an irrigation), even though it has been shown to affect the N-losses to the environment (Phogat et al., 2011). Furthermore, alternative fertigation methods have been suggested including high frequency low-N concentration (HFLC) fertigation. HFLC of different crops has been shown to improve yields, while also minimizing water and N-losses to groundwater (Assouline et al., 2002; Lebese et al., 2014; Silber et al., 2003).

The objective of this work was to investigate whether N leaching to groundwater can be effectively measured using a toolset that monitors water and NO_3^- fluxes just below the root zone; and to apply the toolset to three different BMPs in almond and pistachio orchards. We analyze the spatio-temporal changes in NO_3^- concentrations in both the mobile and immobile soil phases for commercial almond and pistachio orchards as a basis to estimate annual N loss to groundwater. We applied principal component analysis (PCA), chi-squared automatic interaction detector (CHAID), and artificial neural networks (ANN) to evaluate the effect of physical-hydrological parameters on soil NO_3^- concentrations and leaching.

2. Materials and methods

2.1. Study area

The study area is located in Madera County, California, a few kilometers north of the San-Joaquin River (36°49′15.85″N 120°12′1.20″W, Fig. 1), between the towns of Madera and Firebaugh. The site is located in the southcentral portion of the California Central Valley, a large structural trough filled with several thousand meters of older marine and younger continental and alluvial sediments (Page, 1986). Mostly flat, with minimal topographic features, the nearly 60,000 km^2 Central Valley is home to about 3.5–4 million hectares of irrigated lands. The research sites are located on the distal alluvial fan of the San Joaquin River. The two major soil series at the sites are Danube and Cajon sandy loams which consist of deep, moderately to well drained soils (6–14% clay, 67–78% sand) that formed in sandy alluvium from dominantly granitic rocks (SoilWeb, 2015). Duripans (hard-pans) were formed in the region due to pedogenic silica accumulation and flushing of fine soil particles (clay and silt). Weathering and pedological processes created high field scale variability of the degree of cementation and depth to the hard-pan (Kendrick and Graham, 2004; Weissmann et al., 2004). The region's elevation is 50–60 m above sea level. The climate in the region is Mediterranean, with average annual high and low temperatures of 24.2 °C and 9.2 °C, respectively, and an average annual precipitation of 311 mm that falls predominantly during the winter season (November–March). The site is located above a phreatic aquifer, and the depth to the water table is ~30 m below the land surface (BLS). The main recharge to the aquifer is the San Joaquin River, but percolation of seasonal rainwater and leaching of irrigation water from irrigated land also play a role. The region is intensively cultivated with grapes, almonds and pistachios. This area is classified by the California Department of Water Resources as a hydrogeologically vulnerable area (HVA: CDWR, 2000).

Two commercial nut orchards were chosen to study the movement of NO_3^- below the root zone at the orchard scale. The first orchard was a 16 year old, 16 ha (40 acre) almond orchard. Trees are planted on trapeze-shaped berms (0.9 m (3 ft.) wide × 0.2 m high), at intervals of 5.5 m (18 ft.) along the berm and with 7.3 m (24 ft.) driveways between tree rows. The orchard is planted with Nonpareil and Carmel varieties, on alternating rows. The almond orchard consists of a total of 55 rows with 73 trees per row. Each tree is irrigated by one 38–45 L h^{-1} micro-sprinkler (Fan-Jet, Bowsmith, USA), with a 3.5 m wetting radius (total wetted area: 5 ha, 31% of the orchard). The second orchard is a 12 year old, 16 ha (40 acre) pistachio orchard. Trees are planted without a berm 5.2 m (17 ft.) apart with 5.8 m (19 ft.) driveways between tree rows (69 rows of 73 trees). The orchard was planted with Kerman cultivar (Pistacia-vera female cultivar). Each pistachio tree was irrigated with two drip lines of eight 3.8 L h^{-1} drippers, for a wetted area of 1.8 × 5.2 m (total wetted area: 5 ha, 31% of the orchard).

2.2. Fertilizer applications

Three replicates of each of three different fertigation strategies were implemented in a fully randomized complete block design. Each of three blocks consisted of 12 tree rows that extended from the west edge to the center of the orchard. Three fertigation strategies were tested in each block: (i) advanced grower practice BMP (AGP)), (ii) Pump and Fertilize (P&F) which is similar to AGP, but with lower N loads in each fertigation, by accounting for irrigation-water NO_3^--N as 1:1 equivalent to fertilizer-N and, (iii) a high frequency with low N concentration application (HFLC) that followed available N uptake curves and with the same total annual N load as the P&F treatment (ANUP, 2014). Each fertigation strategy was implemented in four neighboring rows (Fig. 1). The orchards were irrigated with locally pumped groundwater containing a NO_3^- concentration of 35 mg L^{-1} and were fertigated with UAN32 fertilizer (Urea Ammonium Nitrate solution, 32% N by weight). Fertigation followed best management practices (BMPs) guidelines, which recommend three to four fertilizer applications during a growing season (ANM, 2014). The AGP and P&F subplots of the

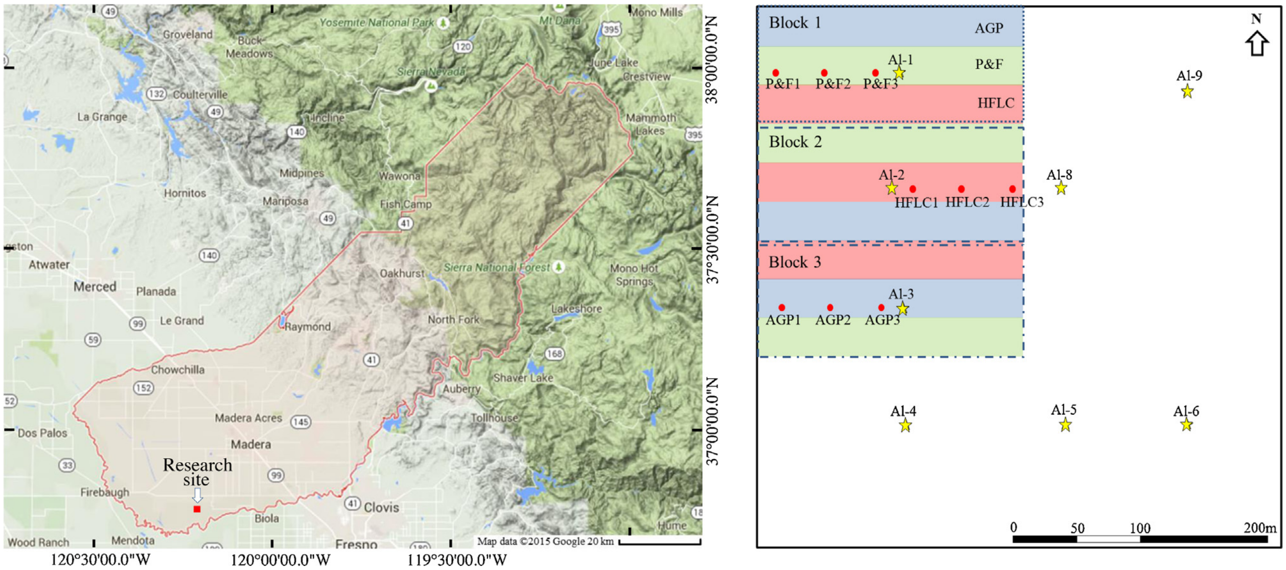

Fig. 1. The location of the research site at Madera county California USA and the monitoring setup at the almond and pistachio orchards.

Table 1
Average nitrogen (N) mass balance for each treatment in the almond and pistachio orchards, for the 2014 and 2015 growing seasons.

	Almond						Pistachio					
	Kg-N ha^{-1}											
	AGP		HFLC		P&F		AGP		HFLC		P&F	
	2014	2015	2014	2015	2014	2015	2014	2015	2014	2015	2014	2015
Inputs												
Fertilizer + groundwater	324	257	324	201	291	201	227	221	207	205	212	205
Compost	45	45	45	45	45	45						
Outputs												
N-in kernel	133	116	146	118	126	124	54	65	53	72	50	83
N-in wood	28	28	28	28	28	28	28	28	28	28	28	28
Hull and shell	76	66	80	67	76	71	23	32	28	36	23	36
Lost	132	91	114	33	107	23	123	96	97	69	110	58
NUE	0.64	0.70	0.69	0.87	0.68	0.91	0.46	0.57	0.53	0.66	0.48	0.72

almond and the pistachio orchards received 50–112 kg-N ha^{-1} and 48 kg-N ha^{-1}, respectively for each fertigation. The HFLC subplots in the almond and pistachio orchards were fertigated every one to three weeks and received 9–12 kg-N ha^{-1} for each fertigation. Total applied N-fertilizer (kg ha^{-1}) for each treatment is presented in Table 1. Nitrogen use efficiency (NUE) was calculated for each treatment as the ratio between tree N uptake (N mass in wood, kernel, shell and hull) and N application (N mass in fertilizer, including organic amendments and groundwater). With this NUE computation, atmospheric N deposition, atmospheric N losses, N in runoff, soil N storage changes, and N losses to groundwater make up the difference between applied and uptake N.

2.3. Monitoring approach and field instrumentation

A grid based soil survey was used to assess the spatial variations in soil layers for both orchards. For that purpose, sixteen boreholes were augured between trees to depth of 3.4 m using a soil hand auger (AMS, ID, USA). Over 230 borehole samples were analyzed for particle size distribution using the hydrometer method (Ashworth et al., 2001). Rooting depth in each orchard was estimated from three 3 m deep soil pits. In the almond and the pistachio orchards most of the roots (>90%) were in the upper 1 m of the profile; few roots were observed below 1 m, visible to a maximum depth of 2.0–2.5 m. Accordingly, hereafter we refer to the upper 1 m of the root system as the 'effective root zone'.

Porewater samplers (solution samplers) and tensiometers were built by attaching round bottom tapered neck ceramic cups (2.2 cm O.D. and 7.0 cm long 1 bar; Soilmoisture Equipment Corp, CA, USA) to 1.905 cm I.D. (3/4 in) to a 0.4, 0.7, 1.0, 1.9, 2.9, 3.0 and 3.1 m long PVC pipes, and attaching a 1.27 cm I.D. (1/2 in), 10 cm long transparent Plexiglas tube to the top. The Plexiglas allowed for real time monitoring of the water level inside the tensiometers, and is sealed at the top by a self-sealing rubber septum. For the tensiometers, an electronic pressure transducer (part No.26PCAFA6D, Honeywell, OH, USA) was connected to the top of the Plexiglas pipe. Flexible (PTFE) electrical spaghetti tubes (0.1 cm I.D.; Cope Plastics, Inc. IL, USA) were guided to the bottom of each solution sampler, allowing porewater sampling using a vacuum pump.

Based on the soil survey information and the observed rooting depth, eight locations were chosen in each orchard for soil layering characterization (Fig. 2). In February 2014 each of those sites was instrumented with five 5TE soil moisture sensors (Decagon, WA, USA), five solution samplers, four tensiometers and a single 3 m long (5.8 cm I.D.) (2 in) PVC neutron probe access tube. The 5TEs and solution samplers were installed at depths of 0.3, 0.6, 0.9, 1.8 and 2.9 m. Tensiometers were installed at depths of 2.8 and 3.0 m, with two at each depth. All instruments were installed inside a 3.175 cm (1–1/4 in) borehole, backfilled with soil slurry and sealed with bentonite along the top 20 cm of the soil. The shallow solution samplers (0.3, 0.6, 0.9 and 1.8 m) and the 5TEs were installed 10 cm apart in a row, parallel to and 1 m away from the center of the berm.

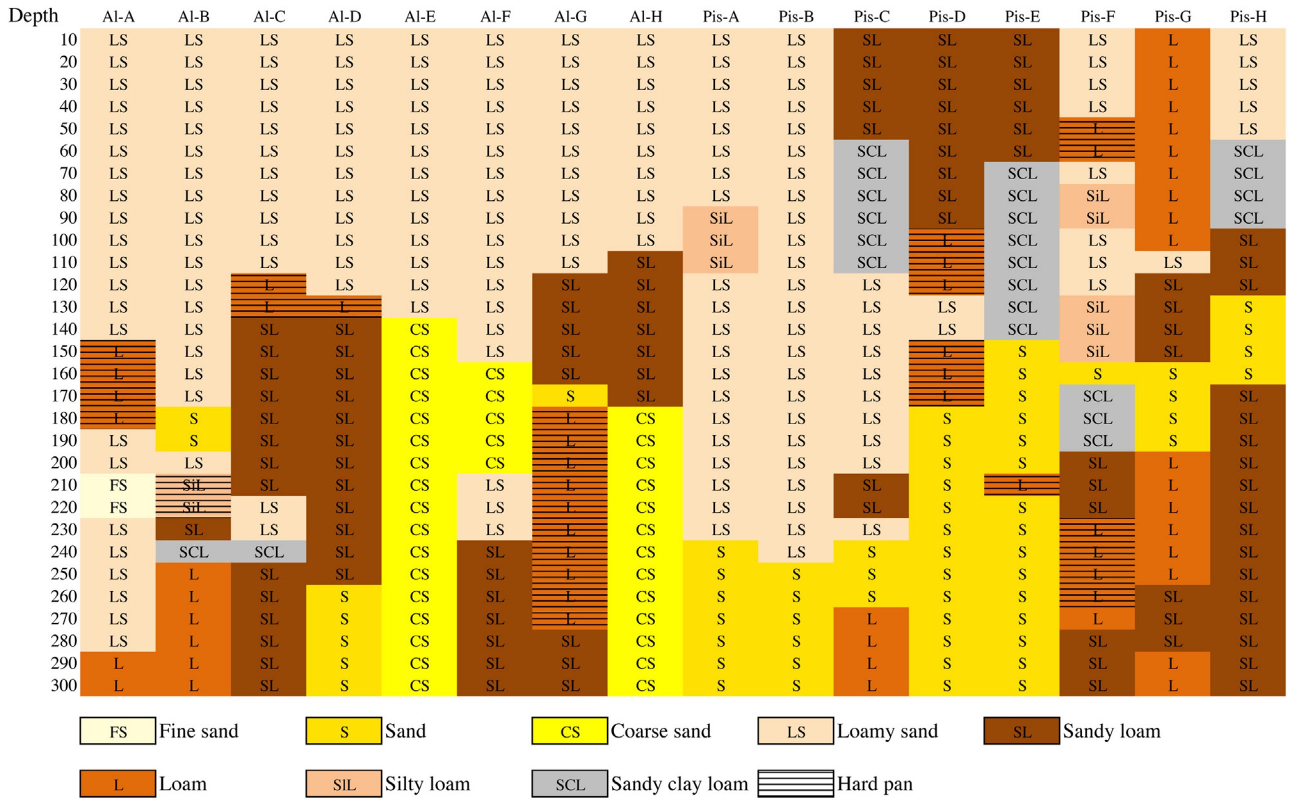

Fig. 2. Soil profiles under the sites (trees) monitored in the almond and pistachio orchards.

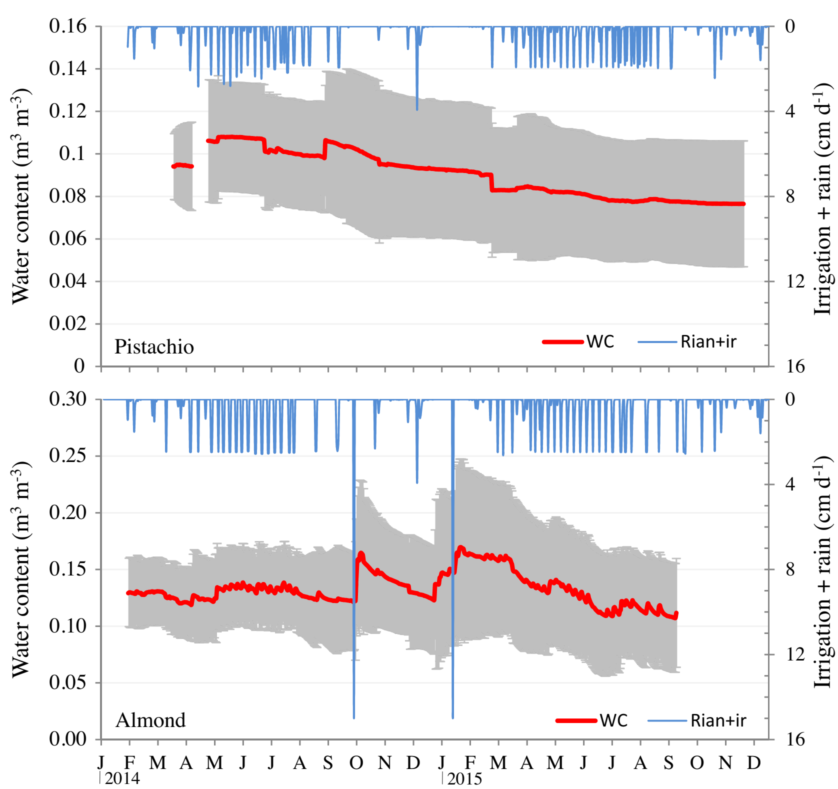

Fig. 3. Temporal trend (2014 through 2015) of average water content at 2.9 m below the pistachio (upper panel) and the almond (lower panel) orchards. Daily average, represents the average of water content readings at the 8 monitoring stations in each orchard. Gray area presents the standard deviation around the average.

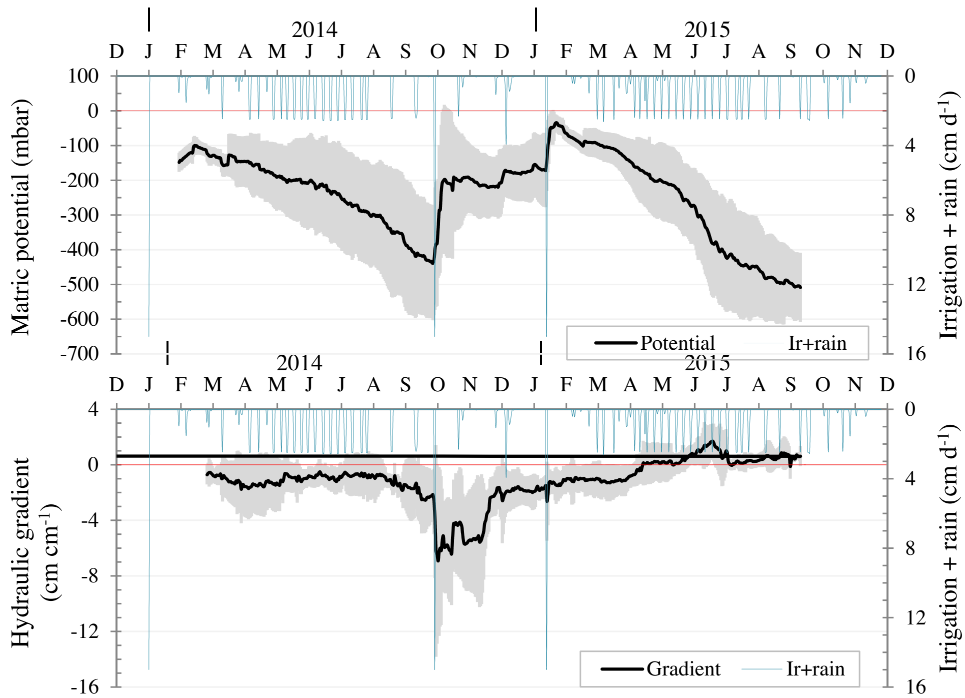

Fig. 4. Temporal changes in average matric potential (upper panel) and the average hydraulic gradient (lower panel) at depth of 2.8 and 3 m below the almond orchard, along with the daily cumulative precipitation. The orchard average matric potential was calculated as the daily average between the readings of the 32 tensiometer installed. The orchard average hydraulic gradient was calculated as the daily average of the average gradient at the 8 monitoring stations. Gray area presents the standard deviation from the average.

The tensiometers were installed 20 cm apart as two couples (2.8 and 3.0 m) located 0.9 and 1.1 m away from the center of the berm, with the deep solution sampler and 5TE (2.9 m) installed between them. A total of nine additional solution samplers were installed at a depth of 2.9 m, three in the AGP treatment row, three in the HFLC treatment row and three in the P&F row (Fig. 1). Porewater was sampled every 1–2 weeks when wet soil conditions extended to depth of 3 m, and up to 4 weeks apart when the soil at depth of 3 m was dry. Following each fertigation event porewater was sampled for three consecutive days. To minimize the effect of porewater sampling on the adjacent tensiometers readings, porewater was sampled after applying suction to the solution sampler for 3–12 h. Neutron probe (model 503DR, CPN, CA, USA) readings were taken using 0.3 m depth intervals, every 1–4 weeks. The neutron probe readings were converted to volumetric water content using a calibration curve that was determined from 45 undisturbed core samples (coefficient of determination $R^2 = 0.96$). Weekly leaching (L) was calculated based on water mass balance:

$$L = (Ir + rain) - (ET_c) - (\Delta S) \tag{1}$$

where *Ir* and *rain* are the cumulative weekly irrigation and precipitation, respectively (cm), ET_c is the cumulative weekly water loss through evapotranspiration (cm) and ΔS is the change in soil water storage over a week (cm). ET_c was estimated based on ET_o data from California Irrigation Management Information System (CIMIS 2014) station 188, which was multiplied by crop coefficients (K_c) based on the work of Goldhamer (2005, 2012).

Mobile water content in the 1.5 m–3.0 m depth interval was calculated based on the assumption that the mobile phase is represented by the N concentrations in the porewater samples (C_{mobile}), and it is associated with the mobile water content (θ_{mobile}), while the total N storage (mobile plus immobile) is represented by soil extractions. We note that:

$$\Delta C_{mobile} = 4.43E6 \times \Delta m_N / (V_{soil} \times \theta_{mobile})$$

Rearranging gives:

$$\theta_{mobile} = 0.738 \times \Delta m_N / \Delta C_{mobile} \tag{2}$$

where θ_{mobile} is the volumetric mobile water content [−], 4.43E6 is a conversion factor from mg NO_3^--N to kg NO_3^-, ΔC_{mobile} is the change in average NO_3^- concentration within the soil volume [mg L^{-1}], Δm_N is the change in NO_3^--N mass within the soil volume [kg N], V_{soil} is the soil volume of 1 ha over 0.6 m depth [m^3] = 6E + 06 [L] = 1 [ha] x 0.6 [m] = 6000 [m^3].

All the tensiometers and 5TE sensors were connected to CR1000 (Campbell Scientific, UT, USA) and NeoMote (Metronome Systems LLC, CA, USA) data loggers. Water content and tension readings were taken every 15 min throughout the year.

Soil water samples were collected every 4–8 weeks. Irrigation water was collected in vials connected to drippers along the irrigation lines for the AGP, P&F and HFLC treatment rows. All water samples were stored in polypropylene bottles and kept on ice until laboratory analysis for NO_3^-, NH_4^+ and total nitrogen after passing through a 45-μm glass fiber filter.

Soil samples were collected prior to the beginning of each growing season (February 2014 and 2015) to determine the total-N content to a depth of 3 m at 30–50 cm depth intervals. Three locations were sampled at each treatment (P&F, AGP, HFLC). The soil samples were extracted with 2 M KCl on 1:2 soil to KCl volume ratio (i.e. 0.02 and 0.04 L, respectively) (Maynard et al., 2008).

All water samples and soil leachates were analyzed for NO_3^- concentrations using vanadium(III) reduction (Doane and Horwáth, 2003); NH_4^+ concentrations as indophenol blue complex using salicylate (Kempers and Kok, 1989) and total-N concentrations using the persulfate digestion method (APHA 4500-N C) (APHA, 1998).

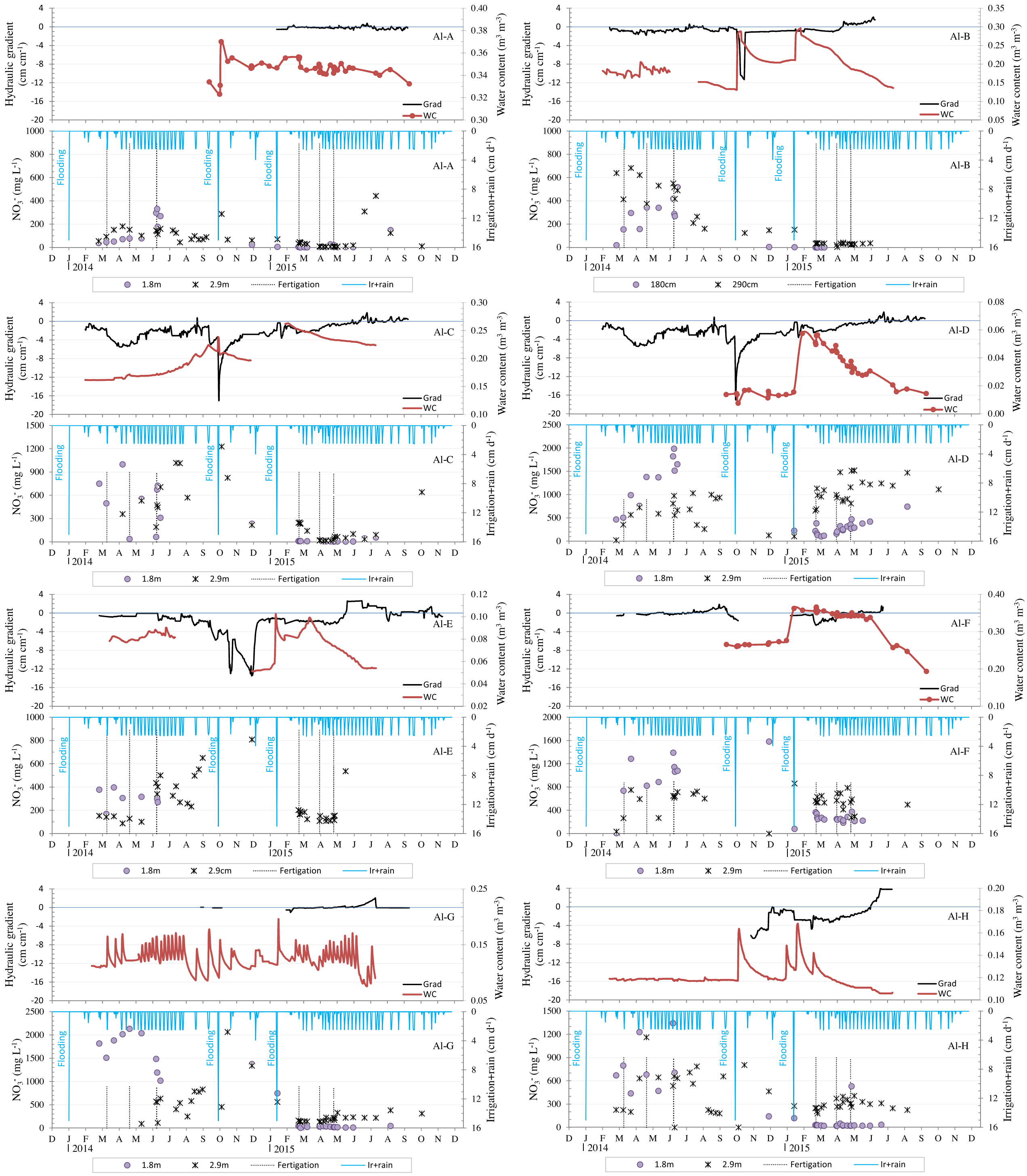

Fig. 5. Temporal changes in NO_3^- concentrations, water content and hydraulic gradient below the root zone at the eight monitoring sites in the almond orchard (Al-A through Al-H), along with the daily precipitation.

2.4. Statistical analysis of NO_3^- concentrations at the 2.9 m soil depth

Statistical analysis was used to examine the relationship between the primary soil physical-hydrological parameters, fertigation treatment, and porewater NO_3^--N concentrations at a depth of 2.9 m, over 1 m below the effective root zone. Parameters considered were (i) hard pan depth (HPD, cm), (ii) thickness (HPT, cm), (iii) and its presence or absence (HP, 0/1), (iv) fertilizer application timing (FAT: middle (1) or end (0)), (v) time after the most recent fertigation (TAF, d), (vi) most recent irrigation duration (ID; h), (vii) occurrence of flooding (FLOOD, 0/1), and (viii) presence of clayey soil at the 290 cm soil depth (CL, 0/1). For the statistical analysis, precipitation events were treated as "irrigation" if they exceeded at least 5 mm and the "irrigation duration" of these events was set to 24 h. The flooding variable (FLOOD) was set to "1" for all measurements that occurred during (and 30 days after) the October 2014 and January 2015 flood irrigations.

Principal component analysis (PCA) (Pearson, 1901) and Chi-squared Automatic Interaction Detector (CHAID) (Kass, 1980) methods were performed using XLSTAT-2015 program (Addinsoft, 2015). PCA was used to assess the strength of the linear relationships (r – correlation coefficient) between the NO_3^--N concentrations and the listed soil hydrological parameters. In addition, the contribution of each of the main parameters to NO_3^- variability was analyzed using both PCA and CHAID. In the CHAID analysis the physico-hydrological parameters (predictor variables) were used to predict if the NO_3^--N concentrations (exploratory variables) could be split, based on these predictors, to a statistically significant discrimination of the dependent variable. To decrease the size of the predictive tree we used the log of the NO_3^--N concentrations and grouped the porewater samples into low ($0.01 \geq 0.5$) intermediate ($0.5 \geq 1.5$) and high ($1.5 \geq 2.5$) concentrations.

An Artificial Neural Network (ANN) analysis was applied to evaluate the relationship and sensitivity between NO_3^--N concentrations from the 2.9 m porewater samples (target output, denoted as N_{cc}) and the same hydrological parameters listed above as input variables. In total, 380 observations were available for each of these variables. We used the MATLAB Neural Network toolbox (MathWorks, 2012), selecting 60% of the NO_3^--N concentration data for ANN training and the remaining 40% for validation purposes. The tested quantities of hidden neurons in the hidden layer were 10, 20, 30 and 40. Note that the number of parameters in the ANN increases with the number "n" of neurons in the hidden layer following a "5n + 1" rule, hence the tested ANNs included 51, 101, 151 and 201 parameters, respectively. To evaluate the optimum number of hidden neurons, and to minimize non-uniqueness and local minima issues, we conducted an optimization stage, running 1000 ANN optimizations for each of 10–40 hidden neurons, using independent initial parameter guesses and compositions of the training dataset. In all cases, ANNs with 40 hidden neurons resulted in the best median validation performance. Hence, the remainder of the analysis focused on results from ANNs with 40 neurons.

Since the average prediction of several ANNs can be more accurate than the prediction of any individual ANN included in the average (Perrone and Cooper, 1993), a bagging method was used to minimize the root mean squared error (RMSE) of the average predictions (Breiman, 1996) of the best ANNs, as follows:

$$\hat{N}_{cc,\,bag} = \frac{1}{B}\sum_{i=1}^{B}\hat{N}_{cc,\,i} \tag{3}$$

where $\hat{N}_{cc,\,bag}$ is the bagged estimator of N_{cc}, $\hat{N}_{cc,\,i}$ is the i^{th} best individual ANN estimator of N_{cc}, and B is the total number of best ANN's selected for the bagging method (the value of B is set to minimize the root mean square error (RMSE) of the bagged estimator; B was 32 on average in this study). The RMSE is defined as:

$$\mathrm{RMSE} = \sqrt{\frac{1}{M}\sum_{j=1}^{M}\left(\hat{N}_{cc,\,bag,j} - N_{cc,\,meas,j}\right)^2} \tag{4}$$

where $N_{cc,\,meas,j}$ is the j^{th} measurement of N_{cc} and M is the total number of N_{cc} measurements. Sensitivity analysis was performed by repeating the same steps once with all the variables and eight more times after removing one input variable each time. Variables whose removal resulted in an increase of RMSE can be considered as most informative on the N_{cc}.

Table 2
Water balance for the orchards.

	Almond		Pistachio	
	2013/14	2014/15	2013/14	2014/15
Rain (mm)	102.2[a]	115.6[a]	102.2[a]	115.6[a]
Irrigation (mm)	1122	1200	723	776
Evapotranspiration (ETc) (mm)	1229[b]	1270[b]	1052[c]	1092[c]

[a] Based on data from CIMIS 2014 station 188.
[b] Using crop coefficients (Kc) from Goldhamer (2012).
[c] Using crop coefficients (Kc) from Goldhamer (2005).

3. Results

3.1. Fertigation

During each growing season, the AGP and P&F subplots were fertigated three times in the almond orchard and four times in the pistachio orchard. The HFLC subplots were fertigated twenty times. In the almond orchard, across treatments, N application amounts in 2015 were about one-third lower than in 2014 (Table 1). In the pistachio orchard, N application amounts were nearly the same in 2014 and 2015 (Table 1). In 2014, UAN32 fertilizer was applied during the middle of a 24–48 h fertigation event, while in 2015 the fertilizer was applied near the end of the irrigation (all treatments). During fertigation events very high NO_3^- concentrations (>11,000 mg L^{-1}) were measured in the irrigation water and also within the effective root zone following fertigations (>880 mg L^{-1}).

3.2. Precipitation and irrigation

The 2014 and 2015 growing seasons began after exceptionally dry winters (Table 2). From bloom/leafing through pre-harvest (almond) and harvest (pistachio) the orchards were irrigated weekly according to the evapotranspiration demand. From August through mid-September the almond orchard was dried for periods of 20–25 days to enable harvest. Following harvest (October) and prior to the awakening of the dormant trees (January), the almond orchard was flood irrigated to refill the soil profile while the pistachio orchard received no post-harvest irrigation in order to dry the soil profile and prevent winter frost damage to branches (dieback). Total annual precipitation and evapotranspiration in the almond and pistachio orchards were nearly identical between the 2013/14 and 2014/2015 growing seasons (Table 2).

3.2.1. Soil water content, matric potential and hydraulic gradient below the root zone

Deep soil wetting events (>3 m) were observed in the almond orchard following pre-bloom (January) and post-harvest (October) flood irrigations, in most of the eight monitoring locations (Fig. 3). Deep wetting events led to high (less negative) matric potentials (<−100 mbar) and to negative (downward) hydraulic gradients at depth of 3 m (Fig. 4 and Fig. 5). Under such wet conditions the unsaturated soil hydraulic conductivity is relatively high, which may result in significant downward flow. During the early and into the main growing season (May for almond), the deep soil (>2.0 m) under the almond orchard dried out, the matric potential decreased (more negative), the unsaturated hydraulic conductivity became very small, and the hydraulic gradient below the effective root zone approached zero, thus preventing potential leaching of NO_3^- (Fig. 3–5).

Under the pistachio orchard the soil at depth of 2.8–3.0 m remained dry throughout the monitoring period (Fig. 3) and the matric potential exceeded the range of our tensiometers (−650 mbar). Hence, the magnitude or the direction of the hydraulic gradient under the pistachio orchard could not be estimated. Even so, at such dry conditions water fluxes would be

Table 3
PCA based Correlation between NO_3^-N concentrations at 2.9 m and different variables.

Variables	HP	HPD	HPT	TAF	ID	Flood	CL	FAT	No. of sites	No. of samples
With HP		**−0.284**	**−0.115**	−0.057	**0.123**	**−0.305**	**−0.585**	**0.253**	14	324
No HP				0.020	0.191	**−0.364**	**0.454**	**0.249**	3	103
AGP	0.077	−0.102	**−0.175**	−0.039	0.096	**−0.282**	**−0.190**	**0.228**	9	249
HFLC		**−0.573**	**0.575**	−0.034	**0.245**	**−0.407**	−0.124	**0.358**	4	87
P&F				−0.013	**0.285**	−0.076		0.022	4	92
All data	**−0.126**	0.001	**−0.163**	−0.039	**0.132**	**−0.333**	**−0.336**	**0.266**	17	427

HP – hard pan; HPD – hard pan depth; HPT – hardpan thickness; TAF – time after fertigation event; ID – irrigation duration; Flood – flood irrigation; CL – clayey soil at 290 cm; FAT – fertilizer application time (middle/end of irrigation).
Values in bold are different from 0 with a significance level alpha = 0.05.

exceedingly small at 2.9 m soil depth due to very low unsaturated hydraulic conductivities (less than 10^{-4} m d^{-1}).

3.3. Nitrate variability and trends below the root zone

3.3.1. Porewater samples

From February 2014 through November 2015 over a 600 porewater samples were collected from the soil profile below the root zone at depths of 1.8 and 2.9 m across the almond and pistachio field sites. The NO_3^- concentrations below the root zone ranged from <1 mg L^{-1} to over 2400, and up to 11,000 mg L^{-1}, respectively (Fig. 6). For the almond and pistachio orchard, the mean NO_3^- concentration below the root zone was nearly one and two orders of magnitude, respectively, higher than the drinking water standard of 45 mg L^{-1} (Fig. 6). However, due to the dry soil conditions in the pistachio orchard throughout the sampling period, only 35 water samples were collected from 1.8 or 2.9 m, with one-third of all samples coming from a single site with extremely high concentrations (>3400 mg L-1 NO_3^-). Hence, we did not statistically compare NO_3^- concentrations between orchards.

In the almond orchard, post-harvest and winter flood irrigation events led to observable downward flushing of NO_3^- to well below the extended root zone (2.9 m), resulting in much lower NO_3^- in the upper 2.9 m. For most of the porewater monitoring stations the decrease in the NO_3^- concentrations was observed immediately after these irrigation events (Fig. 5). During the summer of 2014, a clear increase in NO_3^- concentrations was observed at depths of 1.8 m and 2.9 m across many sites, although without a corresponding decrease in water content. In contrast, during the summer of 2015, only small increases in NO_3^- concentrations were observed at the 1.8 and 2.9 m depths (Fig. 5).

Under both AGP and HFLC treatments the average NO_3^- concentration at 2015 was significantly lower than in 2014 (397 mg L^{-1} vs. 265 mg L^{-1}, $P = 0.0001$, and 277 mg L^{-1} vs. 14 mg L^{-1}, $P = 0.007$, respectively). In the P&F treatment no difference was observed between the average NO_3^- concentration in 2014 and 2015 (72 mg L^{-1} vs 78 mg L^{-1}, $P = 0.33$) and during both growing seasons the concentration remained low (Fig. 5 Al-1). However, low NO_3^- concentrations were observed at the P&F sites prior to the beginning of the monitoring campaign (Fig. 7); hence these observations cannot be said to represent a significant difference between treatments. Across treatments, at the orchard scale, the average porewater concentration in 2014 was higher than in 2015 (251 mg L^{-1} vs. 135 mg L^{-1}, $P < 0.00001$).

3.3.2. Soil extractions

N mass in soil extractions following the flood irrigation prior to the beginning of each growing season (February 2014 and 2015) showed only small changes in the total soil N-stocks between winter 2014 and winter 2015, with NO_3^- being the most dominant N-form (>95%) (Fig. 7). Within the effective root zone (0–1 m) the N stock prior to the beginning of the 2014 and 2015 growing seasons did not significantly change and remained low (7.2 ± 4.3 and 9.5 ± 3.2 kg-N ha^{-1}, respectively; $P = 0.124$) across all treatments. N-stock in the deeper vadose zone (1–3m) remained high and did not change significantly between 2014 and 2015 (172 ± 100 and 140 ± 99 kg-N ha^{-1}, respectively; $P = 0.247$). The maximum observed total N storage is on the order of 100 kg N ha^{-1} per 60 cm depth interval, typically near the deepest sampling point at 2.9 m (Fig. 7). The largest difference in total N storage below the effective root zone observed between February 2014 and February 2015 is 50 kg N ha^{-1} per 60 cm depth interval or smaller.

3.4. Mass balance

3.4.1. Yield

Harvest yields in the almond orchard varied somewhat between treatments in 2014 (126–146 kg kernel-N ha^{-1}), but were nearly identical (116–124 kg kernel-N ha^{-1}) in 2015. The P&F treatment resulted in similar N-uptake in both years (126 vs. 124 kg kernel-N ha^{-1}), despite the lower N application rate in 2015. The AGP and HFLC had 13% and 20% lower N yields in 2015, respectively.

In the pistachio orchard harvest N yields were about 50–54 kg kernel-N ha^{-1} across treatments in 2014, and increased significantly by 20%, 36%, and 66% for AGP, HFLC, and P&F, respectively in 2015 (Table 1). The decrease in the almond yields and the increase in the pistachio yields in 2015 were in agreement with the alternate bearing trend in the region, and probably did not result from inter-annual differences in the fertilizer loads.

3.4.2. Water leaching below the root zone

Leaching estimates for the almond orchard, based on water mass balance, indicate average rates of 10.4 ± 8.4 cm y^{-1}. The maximum and the minimum observed leaching fluxes were 24.2 and 1.9 cm y^{-1}, respectively. The average leaching from the pistachio was −30 cm y^{-1}; indicating upward flow conditions on most days. This value is lower bound estimate (most negative) due to the use of crop coefficients (Kc) that did not account for the drying of the soil past harvest (Goldhamer, 2005), and the very small unsaturated hydraulic conductivities at that time.

3.4.3. Nitrogen use efficiency (NUE)

Annual mass balance estimates of the NUE (the ratio of tree N uptake to N application) showed an average NUE of 75% and 57% for the almond and the pistachio orchards, respectively, with higher NUE in 2015 than in 2014 (Table 1). The N stock in the effective root zone was not accounted for in the calculations since it was very low and did not change significantly (Section 3.3.2). Higher NUE was measured across all treatments in 2015 when compared to 2014. The largest improvement was observed in the HFLC and P&F treatment in both, almonds and pistachios: there, the NUE increased by about 20%. In the AGP treatment, which had the lowest NUE, the NUE increased by 6% and 11% for almonds and pistachios, respec-

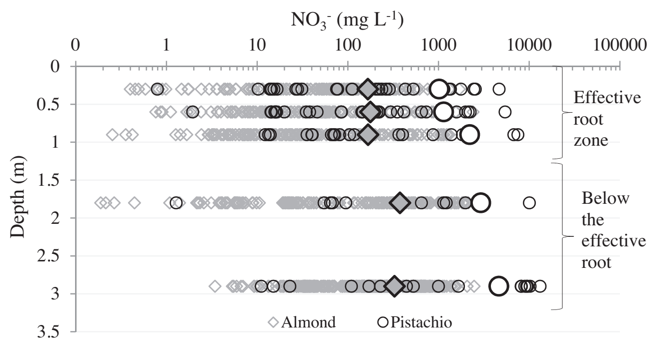

Fig. 6. Nitrate (NO_3^-) concentrations in porewater samples from eight vadose zone monitoring sites in an almond and pistachio orchard, each sampled during the 2014 and 2015 growing seasons. Large symbols represent average concentrations.

Table 4
RMSE of the bagged estimator predictions in ANN analysis after removal of each individual input variable.

Removed variable	RMSE (NO_3^- mg L^{-1})[a]
Hard pan thickness	240
Clayey soil at 290 cm	233
Irrigation duration	227
None	224
Flood irrigation	223
Hard pan	222
Hard pan depth	219
Fertilizer application time	219
Time after fertigation	219

[a] Variables whose removal induced increased RMSE is the most informative on the bagged estimator N_{cc}.

tively; thus, the 2015 NUEs for HFLC and P&F are significantly higher than for the AGP (Table 1).

Average annual N losses to the atmosphere and groundwater were 83 and 92 kg-N ha^{-1} in the almond and the pistachio orchard, respectively (across treatments). More specifically, under current BMPs (represented by AGP), average annual losses were 111 and 110 kg N ha^{-1} in the almond and pistachio orchard, respectively. For HFLC and P&F treatments, average annual N losses were much lower, 69 and 84 kg-N ha^{-1} in the almond and pistachio orchard, respectively.

3.5. Statistical analysis of factors affecting NO_3^- concentrations below the root zone

Correlations between NO_3^- concentration in 427 soil solution samples (collected across the orchards at multiple times at the 2.9 m soil depth) and the presence (HP), thickness (HPT, cm) and depth (HPD, cm) of the hard-pan, sampling times after fertigation (TAF, 0–40 days), irrigation duration (ID, hours), presence or absence of a clayey soil layer at the 2.9 m depth (CL, 0/1), fertilizer application time (FAT, middle (1) or end (0)), and occurrence of flooding events (FLOOD) were all very weak using the Principal Component Analysis (PCA) method ($<r = 0.34$; Table 3). Similarly, in the Artificial Neural Network (ANN) method RMSE's were all relatively large (~50 mg-N-NO_3^- L^{-1}; Table 4) and in the Chi-squared Automatic Interaction Detector (CHAID) analysis, five levels of branching could not identify single variables that could statistically discriminate the NO_3^- concentrations into categories (low ($0.01 \geq 0.5$) intermediate ($0.5 \geq 1.5$) and high ($1.5 \geq 2.5$) concentrations; Supporting information 1 (SI-1)).

The presence of finer soil layer at 2.9 m (CL) was found to be the largest contributor to the dependence on NO_3^- concentration in all three methods (PCA, $r = -0.336$, Table 3; ANN RMSE = 54.2 mg L^{-1}, Table 4; CHAID first split (branching), SI-1). Flood irrigation had a strong to moderate impact on the soil NO_3^- variability.

4. Discussion

4.1. Nitrate variability and trends below the root zone

It is likely that extremely high concentrations observed at the pistachio site stems from the differences in the agricultural water management at both orchards: exceptionally dry winters and the differences in the irrigation management between orchards led to minimal deep leaching and the buildup of much higher NO_3^- concentration below the root zone of the pistachio orchard. Due to the small number of porewater samples collected from that orchard (i.e. 35, from 1.8 or 2.9 m), further discussion in this subsection focuses focus on the observations from the almond orchard.

4.1.1. Timing of fertilizer application

Using the frequent 'snapshot' porewater sampling method, clear differences were observed between the NO_3^- concentrations below the effective root zone in 2014 and 2015 (i.e. clear increase in 2014 and small increases in 2015) (Fig. 5). The latter, plus the similarity between the porewater NO_3^- concentrations at each of the monitoring locations, especially throughout the 2015 growing season, indicates that the sampling method managed to capture the temporal variability in NO_3^- concentrations. Accordingly, the difference in NO_3^- concentrations is thought to reflect the timing of fertilizer application within an irrigation event: in 2014, UAN32 fertilizer was applied during the middle of a 48 h fertigation event, while in 2015 the fertilizer was applied near the end of the irrigation (all treatments). As a result, under both AGP and HFLC treatments the average NO_3^- concentration below the root zone in 2015 was significantly lower than in 2014 (397 mg L^{-1} vs. 265 mg L^{-1}, P = 0.0001, and 277 mg L^{-1} vs. 14 mg L^{-1}, P = 0.007, respectively).

The results are consistent with other studies that have shown that fertilizer losses are closely related to the timing of fertilizer application (Morgan et al., 2007; Neilsen et al., 2001; Phogat et al., 2014; Quiñones et al., 2007). Gärdenäs et al. (2005) showed that fertigation at the beginning/middle of an irrigation cycle under wet soil conditions tends to increase seasonal nitrate leaching, while fertigation events at the end of the irrigation cycle reduces the potential for NO_3^- leaching. It is important to note, that under current BMPs recommendations for almond orchards (i.e., AGP) most (66%) of the N-fertilizer application take place early in the growing season (March–April) when wet soil conditions, downward gradients, and high unsaturated hydraulic conductivity prevail to soil depth exceeding 3 m (Fig. 5). Accordingly, it is very likely that most of the N-losses occur during that time period (March–April). The positive correlations between porewater NO_3^- concentrations and the time after fertigation (TAF) in the PCA analysis, for all fertigation treatments (Table 3), corroborates the recommendation to preferably apply fertilizer towards the end of an irrigation event, as well as to apply water using high frequency and short duration so as to maintain the applied fertilizer and water in the root zone (<1 m).

Fig. 5 Al-D, shows an example, where NO_3^- concentration at 290 cm increases in the 2015 growing season, even though the fertilizer was applied at the end of all irrigation events. It is possible that downward gravity flow following fertilizer-N application at the end of an irrigation event leads to deep fertilizer transport, mainly due to reduced lateral distribution by capillary movement (Cote et al., 2003). This may be the case in particular early in the season when the soil is wet and negative gradient prevails below the effective root zone (Fig. 4). Once NO_3^- moves past the effective root zone (>1 m), low organic carbon content, low microbial activ-

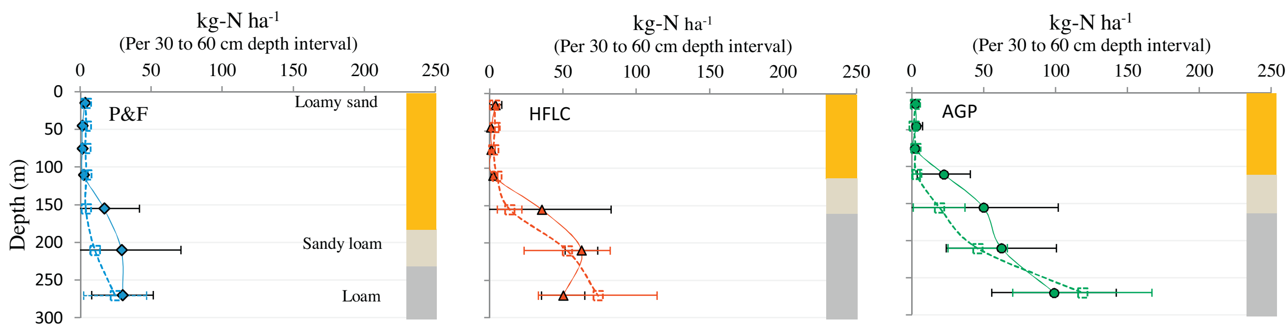

Fig. 7. Nitrogen quantities (Kg-N ha^{-1}) in the soil profile under the almond orchard in Madera at February 2014 (full symbols) and February 2015 (hollow symbols). All the values were normalized to the water content and represent integration of 30–50 cm intervals. The left panel represents sampling sites under the P&F treatment, the middle panel represents locations under the HFLC treatment and the right panel represents locations under the AGP treatment. The lithological profile at each site is presented at the right side of each panel.

ity, and minimal root N uptake minimizes the attenuation of NO_3^- leaching.

Unlike in early season fertilizer application, late season application (May – June) did not lead to a clear increase in the NO_3^- concentrations, and only small changes in the NO_3^- concentrations are observed throughout the summer of 2014 and 2015. Beginning in May, when the hydraulic gradients and unsaturated hydraulic conductivities below the effective root zone become negligibly small with negligible vertical flow, the water content decreased drastically without a commensurate increase in NO_3^- concentrations (e.g., Fig. 5 A1-B, A1-D, A1-E, A1-F, A1-H). This strongly suggests that the decrease in water content was due to root water uptake, and perhaps due to limited upward movement of soil water including its dissolved NO_3^-. Therefore, the decrease in soil water content below the effective root zone during the summer does not concentrate the NO_3^- that remains in solution and possibly extends the effective root zone via wicking to well below 1 m. An additional indication that applied fertilizer and water ARE not reaching the 2.9 m soil depth during most of the growing season (i.e. May through Oct) comes from the low contribution of TAF to the variability in the porewater NO_3^- concentrations (Table 3 and Table 4).

The HFLC method (especially when combined with a P&F approach), which uses frequent short fertigation events, may better keep water and NO_3^- preferentially in the effective root zone (<1 m) especially when irrigating frequently (few times a week) at rates corresponding to plant uptake needs (Phogat et al., 2011, 2014). This has significant advantages over conventional Californian practices where micro-irrigation is applied once a week continuously for 24–48 h and fertilizer is applied 3–4 times in large loads (AGP). With an irrigation height of 1000 mm, an NUE of 70%, and N uptake of about 220 kg-N ha^{-1} (almonds) and 110 kg-N ha^{-1} (pistachios), concentrations in fertigation water, if N is applied continuously with all irrigations (maximum dilution), would be on the order of 135 and 68 mg NO_3^- L^{-1}, respectively. If fertigation is limited to the last third of the duration of an irrigation event and to one fifth of all irrigations, the NO_3^- concentration of the fertigated water must be increased 15-fold to 2000 and 1000 mg NO_3^- L^{-1} to deliver the same amount of N (http://www.ucanr.org/sites/Kern22/files/98609.pdf). Indeed, we observe very high NO_3^- concentrations observed in the irrigation water during fertigation (>11,000 mg L^{-1}) and also within the effective root zone following fertigation (>880 mg L^{-1}). These high concentrations possibly exceed the maximum concentration that can be absorbed by the tree roots. This may further increase NO_3^- losses through leaching to below the effective root zone (Kurtzman et al., 2013; Shapira, 2012), even at times when there is an N deficit in the plant. To the best of our knowledge, the maximal NO_3^- concentration taken up actively or passively by almond and pistachio roots has never been determined. This supports the paradigm that a transition from flood irrigation to micro-irrigation has the highest potential to reduce the risk of groundwater NO_3^- pollution only by adapting to high frequency fertigation practices, with irrigation water NO_3^- closely matching root NO_3^- uptake during the irrigation season (Dzurella et al., 2015). Further research on tree root uptake potential limited by NO_3^- concentrations in the irrigation water may be helpful to prevent use of excessive NO_3^- concentrations in fertigation.

Table 5
Correlations (factor loadings) between variables and principal components (PC) for all the data.

	PC1	PC2	PC3	PC4	PC5
[a]*Variability (%)*	*34.6*	*16.7*	*12.4*	*9.4*	*8.3*
NO_3^--N	−0.368	0.307	−0.320	**−0.631**	−0.170
Hard pan	**0.872**	0.327	−0.170	−0.132	−0.032
Hard pan depth	**−0.819**	−0.328	0.178	0.319	0.034
Hard pan thickness	**0.733**	0.288	−0.197	0.272	−0.129
Time after fertigation	−0.033	0.431	**0.758**	−0.006	0.119
Irrigation duration	−0.123	**0.674**	0.420	−0.053	0.319
Flood irrigation	**0.652**	−0.509	0.411	−0.212	−0.069
Fertilizer application time	**−0.559**	**0.609**	−0.362	0.129	0.161
Clayey soil at 290	**0.679**	0.196	−0.121	**0.534**	0.022

Note: Bold values represent the variables with the main influence on each principal component.
[a] Represents how much (%) of the initial variability is represented by each PC.

4.1.2. Field scale nitrogen fluxes

Using PCA, the main and second principal components (PC1 and PC2, Table 5) could explain at most 50% of the variability in the porewater NO_3^- data. Similarly, even after four levels of statistically significant discriminations, the CHAID analysis could not explain the variability in the data (as suggested by the purity degree in each node (SI-1)). The PCA suggested that NO_3^- loses to the deep profile decrease when the thickness of the HP increases ($r = -0.163$; Table 3). However, it is likely that the cause of the small dependence between the presence of hard pan (HP) in the subsurface and the NO_3^- leaching ($r = -0.126$; Table 3) comes from field scale variability in depth and degree of cementation of the hardpan (Fig. 2), as also documented by Kendrick and Graham (2004) and Weissmann et al. (2004). Overall, our statistical analyses show that a large proportion of NO_3^- concentration variability could not be explained by soil characteristics, suggesting additional parameters not considered in this study, such as water application nonuniformity and sampling location relative to the emitters (Rolston et al., 1991), as well as spatial variations in root nutrient and water uptake rates within and between trees estimated to spatially vary by 5–8% in a similar almond orchard (Couvreur et al., 2016).

The statistical analysis suggests that much of the variability can be treated as "white noise" with average concentrations across sites being the most meaningful statistic at the plot or field scale. Indeed, despite the large spatial and temporal variability observed in porewater NO_3^- concentrations, average porewater concentrations are consistent with annual N losses obtained from the N mass balance (83 kg N ha^{-1}): when multiplying porewater concentrations, which average 80 mg NO_3^--N L^{-1} at 2.9 m, with the annual average recharge rate of 0.1 m y^{-1}, total annual N in recharge amounts to 80 kg N ha^{-1}.

4.2. Mobile vs. immobile NO_3^-

4.2.1. Indications

Both, water and nitrogen mass balances, and the temporal dynamics of porewater NO_3^- after fall and winter irrigations (Fig. 5) indicate significant losses of NO_3^- to below 3 m, which is below the uptake zone of tree roots. Yet, N mass in soil extractions following the flood irrigation prior to the beginning of each growing season (February 2014 and 2015) showed only small changes in the total soil N-stocks between winter 2014 and winter 2015 (Fig. 7). Integration of the NO_3^--N stock between 1.5 m and 3.0 m (below the effective rooting zone) indicates a field-average of about 132 kg NO_3^--N ha^{-1}. This is equivalent to more than 55% of the total annual N amount suggested by current BMP guidelines to support good commercial crop yields in both the almond and pistachio orchards. Field observations of rooting depth and density indicate that most roots (>90%) are located in the upper 1 m of the soil profile (Koumanov et al., 2006). It is therefore – at best – unknown and possibly unlikely that much of the large N pool observed at 1.5 m–3.0 m depth is plant available. Based on NUE this NO_3^--N stock represents about 1.5 years of total N losses (Table 1). Assuming that some of the computed N losses in Table 1 are to the atmosphere, the measured pool likely represents 2 or more years of N losses to groundwater.

While soil core extractions in winter 2014 and winter 2015 show little N variability in time, the NO_3^- concentrations observed in the pore water samplers (suction lysimeters) at the 1.8 m and 2.9 m depth differ generally by several tens mg–L^{-1} to over 500 mg L^{-1} within the same time period, ranging from less than 100 mg L^{-1} to well over 1000 mg L^{-1} (Fig. 5). The differences in nitrogen dynamics between total soil core extraction and soil solution porewater suggest the presence of two separate NO_3^- pools, a mobile and an immobile NO_3^- pool. Soil core extraction includes both the mobile and immobile soil N pools, whereas the pore water solution obtained by suction lysimeter includes only the mobile pool.

The much larger variability of the pore water samples (Fig. 5and 6), especially in 2014, when compared to the changes observed in total N storage (Fig. 7) may have two explanations: First, pore water NO_3^- concentrations represent most of the total N store and do not change much when averaged (corresponding to Fig. 7) but are highly variable individually (Fig. 5 are individual samples). Second, the large range of concentrations observed in Fig. 5 corresponds to an overall small change in soil N store because most of the 132 kg N ha^{-1} in the soil storage is contained within the immobile phase.

We tested the first hypothesis by testing whether the average concentrations at 2.9 m depth are statistically significantly different between February–March 2014 and February–March 2015, given the large variability in time. Using t-Test (not shown), results show that average mass stored in the soil (mobile + immobile) remained significantly higher than the mass contained in the porewater ($P = 0.012$ and $P = 0.008$, respectively). These results suggest that despite the deep wetting following the flood irrigation, a significant immobile N pool remains and dominates the total N storage at 1.5–3.0 m depth after these irrigations.

Additional indication to the presence of mobile and immobile N-pools came from using Eq. (2). As an upper bound, taking into account the largest difference observed in total N storage between February 2014 and February 2015 ($\Delta m_N = 50$ kg N ha^{-1} per 60 cm depth interval) and the corresponding average change in pore water concentration ($\Delta C_{mobile} = 100$ mg NO_3^- L^{-1}), would reflect a mobile water content of 37%. This water content is higher than any measured water content in February and March, which were measured to range from about 5% to about 30%, with most samples exceeding 10% (Fig. 5). Alternatively, if average change in pore water concentrations are assumed to be on the order of 300 mg NO_3^- L^{-1} (also consistent with Fig. 5) representing 10 kg N ha^{-1} per 60 cm depth interval total average N storage change (consistent with Fig. 7), the mobile water content is 2.5%, or about one-third to one-tenth of the total measured water content. The February 2014 to February 2015 changes in pore water NO_3^- concentrations and in total soil N storage therefore suggest mobile pore water is likely a fraction of the total water content, ranging anywhere from less than 3% volumetric content to nearly the full water content (less than 10% to over 20%).

The statistical analysis provided additional indication to the presence of mobile and immobile N-pools. In the PCA analysis, the presence of clayey soil layer at the 2.9 m (CL) was negatively correlated to the porewater NO_3^- concentrations (Table 3); indicating, in contrast to the soil extractions (Fig. 7), that the presence of clayey soil layer at the 2.9 m depth does not restrict NO_3^- movement and does not lead to NO_3^- accumulation. Similar to the PCA, and in contrast to the soil extractions, CHAID analysis indicated that 83% of the intermediate (log NO_3^--N concentrations $0.5 \geq 1.5$) and 96% of the low NO_3^- concentrations (log NO_3^--N concentrations $0.01 \geq 0.5$), were found in porewater samples taken from locations with clayey soil at the 2.9 m soil depth (SI-1). It is possible that these negative correlations resulted to some extent from NO_3^- losses due to denitrification in anaerobic microsites in the clayier soil layer. Yet, this process was probably limited, as suggested in other studies on subsurface microbial denitrification activity (Brye et al., 2001).

4.2.2. Implications

If mobile pore water represents nearly all of the total water content (upper bound) and piston flow conditions dominate, the effective vertical travel velocity of NO_3^- at these sites, under the conditions shown here for 2014–2015, is less than 1 m per year. This suggests a half century-long travel time to the water table at 30 m depth at these sites, under 2014–2015 conditions. NO_3^- concentrations reaching the water table would be very high at the water table assuming they remain unchanged from those at 1.5 m–2. 9 m depth (Fig. 5), absent of significant denitrification in the deeper vadose zone. However, over the long travel time in the vadose zone, even relatively small denitrification rates (on the order of 3%–5% per year), if present, have the potential to decrease measured high concentrations10 to 20-fold, to below the drinking water limit, before reaching the water table.

On the other hand, if N storage of 132 kg ha^{-1} in the 1.5 m – 3.0 m zone represents mostly immobile N, it likely accumulated over several years to decades and, in that case, would represent only a small fraction of the total N losses that have occurred over the same period, given the above estimates of annual N losses to below the root zone. The large changes in mobile water N reflects rapid transport of N in a relatively small fraction of the water volume, suggesting that much of the annual N losses (Table 1) may reach the water table within less than a decade, at relatively high concentration.

The presence of a large N pool below the root zone has practical consequences: High rainfall or irrigation rates during the winter may lead to a flushing of the N pool. This may also limit practices to replenish groundwater in California's Central Valley by deliberately flooding dormant nut orchards with excess stream flow during winter storms, unless sufficiently diluted or unless the pool remains immobile. All three statistical methods used by us, highlighted the contamination potential associated with extreme wetting events, by showing strong to moderate impact of flood irrigation on porewater NO_3^- variability (Tables 3 and 4, and SI-1).

Differences between solution sampling versus soil extraction techniques are consistent with Landon et al. (1999) and Baram et al. (2013). The differences in concentrations between the two sampling methods there were attributed to most of the applied N-fertilizer or solutes remaining in the mobile pool, and therefore more likely to be transported deeper into the vadose zone and into groundwater. Similarly, deep (15 m) vadose zone NO_3^- profiles under a flood-irrigated nectarine orchard, were explained by rapid preferential movement of N in a mobile zone that constitutes about 3–5% volumetric water content, while total water content averaged 20% (Botros et al., 2012; Onsoy et al., 2005). Such rapid mobile flow is likely due to local soil textural and structural differences that leads to preferential flow, such as by fingering (Hillel, 1998; Vogel et al., 2000), lateral/funneled flow (Walter et al., 2000) or thereby further preventing the leaching of solutes. Such phenomenons are enhanced typically by field scale variations in degree of cementation and depth.

For our fall and winter flood irrigations, differences in NO_3^- concentrations below the orchards observed between sampling methods and temporal trends in the pore water samples indicate that these high volume irrigations do not uniformly flush salts from the soil profile due to spatially heterogeneous fluxes. Furthermore, the comparison of pore water NO_3^- concentration following two flood irrigations at the 2.9 m depth in Fig. 5 Al-F shows no flushing of NO_3^-, although the wetting front reached the 2.9 m soil depth. Such observations are in agreement with other experimental studies on solute transport in the vadose zone after surface flooding (Amiaz et al., 2011; Dahan et al., 2008). These studies suggest that wetting fronts do not move through the soil as piston flow during and after flood irrigation. Significant fractions of dissolved ions such as salts and NO_3^- remain in the soil and are not necessarily transported deeper in the vadose zone. It remains unclear, whether these accumulate only over long periods of time or, in fact, represent a significant fraction of annual solute fluxes.

5. Conclusions

The data presented in this manuscript showed tremendous spatial and temporal variations in deep soil NO_3^- concentrations in almond and pistachio orchards, regardless of irrigation practices. Yet, using intensive instrumentation data yielded significant results annual leaching of N at the orchard scale. Comparison of mass balance estimates for water and N indicated that the annual orchard average N loss can be estimated based on averaging data from eight monitoring sites. Results further indicated that soil cores taken prior to the beginning of the growing season; represent a largely immobile N pool that is unrelated to actual N losses. In contrast, porewater samples (suction lysimeters) provide a snapshot of concentration profiles immediately below the root zone, where NO_3^- is subject to leaching to the water table, at possibly rapid speed and within a small fraction of the porous media.

Current BMPs for fertigation guidelines caused very high NO_3^- concentrations in and below the root zone, likely exceeding maximum root NO_3^- uptake rates. Statistical analyses of deep soil NO_3^- concentrations showed that knowledge of bulk soil physical properties and their field variations was not sufficient to characterize orchard-scale leaching. It also indicated that most of the N loss occurred through preferential flow, measured by porewater samplers. Preferential flow in turn may limit practices that might replenish groundwater in California's Central Valley such as deliberate flooding of dormant nut orchards with excess stream flow during winter storms, unless sufficiently diluted. These results indicate that irrigation water management practices are as critical as nitrogen application management practices. Implementation of alternative water and N-fertilizer application methods, such as HFLC, are required to control NO_3^- leaching and to protect groundwater. Such new practices will need to include knowledge of optimal root N-uptake rates so that fertigation rates and frequencies can be adjusted to minimize nitrate leaching.

Acknowledgments

We acknowledge funding from the California Department of Food and Agriculture's Fertilizer Research and Education Program (CDFA-FREP) through project 12-0454-SA, by the Almond Board of California through project number 13PREC6SMART and by the California Pistachio Research Board through project number 2013-02890. During the preparation of this manuscript, V.C. was supported by the "Belgian American Educational Foundation" (BAEF) as UC-Louvain Fellow, by "Wallonie-Bruxelles International" (WBI) with a WBI.WORLD excellence grant, and by the "Fonds Spéciaux de Recherche" (FSR) of the Université catholique de Louvain.

Appendix A. Supplementary data

Supplementary data associated with this article can be found, in the online version, at http://dx.doi.org/10.1016/j.agwat.2016.04.012.

References

Addinsoft, 2015. XLSTAT, 2015, Data analysis and statistics software for Microsoft Excel.
Allaire-Leung, S.E., Wu, L., Mitchell, J.P., Sanden, B.L., 2001. Nitrate leaching and soil nitrate content as affected by irrigation uniformity in a carrot field. Agric. Water Manage. 48, 37–50, http://dx.doi.org/10.1016/S0378-3774(00)00112-8.
Amiaz, Y., Sorek, S., Enzel, Y., Dahan, O., 2011. Solute transport in the vadose zone and groundwater during flash floods. Water Resour. Res. 47, 1–10, http://dx.doi.org/10.1029/2011WR010747.
ANM, 2014. Almond Nitrogen Model (ANM) [WWW Document] (accessed 8.20.15) http://ucce.ucdavis.edu/rics/fnric2/almondNKmodel/almond_model.html.
ANUP, 2014. Almond Nitrogen Uptake and Partitioning (ANUP) [WWW Document] (accessed 8.20.15) http://apps.cdfa.ca.gov/frep/docs/N_Almonds.html.
APHA American Public Health Association), 1998. Standard Methods for the Examination of Water and Wastewater, 20th ed. United Book Press, Baltimore, MD.
Ashworth, J., Keyes, D., Kirk, R., Lessard, R., 2001. Standard procedure in the hydrometer method for particle size analysis. Commun. Soil Sci. Plant Anal. 32, 633–642, http://dx.doi.org/10.1081/CSS-100103897.
Assouline, S., Cohen, S., Meerbach, D., Harodi, T., Rosner, M., 2002. Microdrip irrigation of field crops: effect on yield, water uptake, and drainage in sweet corn. Soil Sci. Soc. Am. J. 66, 228–235.
Baram, S., Ronen, Z., Kurtzman, D., Külls, C., Dahan, O., 2013. Desiccation-crack-induced salinization in deep clay sediment. Hydrol. Earth Syst. Sci. 17, 1533–1545, http://dx.doi.org/10.5194/hess-17-1533-2013.
Böhlke, J.K., 2002. Groundwater recharge and agricultural contamination. Hydrogeol. J. 10, 153–179, http://dx.doi.org/10.1007/s10040-001-0183-3.
Botros, F.E., Onsoy, Y.S., Ginn, T.R., Harter, T., 2012. Richards equation-based modeling to estimate flow and nitrate transport in a deep alluvial vadose zone. Vadose Zone J. 11, http://dx.doi.org/10.2136/vzj2011.0145.
Breiman, L., 1996. Bagging predictors. Mach. Learn. 24, 123–140, http://dx.doi.org/10.1023/A:1018054314350.
Brye, K., Norman, J., Bundy, L., Gower, S., 2001. Nitrogen and carbon leaching in agroecosystems and their role in denitrification potential. J. Environ. Qual. 30, 58–70.
CDFA, 2014. California Department of Food and Agriculture). 2014California Almond Acreage Report [WWW Document] (accessed 9.9.15) http://www.nass.usda.gov/Statistics_by_State/California/Publications/Fruits_and_Nuts/201504almac.pdf.
CDWR, 2000. California Department of Water Resources). Hydrogeologically Vulnerable Areas Map [WWW Document] (accessed 8.20.15) Http://www.waterboards.ca.gov/gama/docs/hva_map_table.pdf.

Cote, C.M., Bristow, K.L., Charlesworth, P.B., Cook, F.J., Thorburn, P.J., 2003. Analysis of soil wetting and solute transport in subsurface trickle irrigation. Irrig. Sci. 22, 143–156, http://dx.doi.org/10.1007/s00271-003-0080-8.
Couvreur, V., Kandelous, M.M., Sanden, B.L., Lampinen, B.D., Hopmans, J.W., 2016. Downscaling transpiration rate from field to tree scale. Agric. For. Meteorol. 221, 71–77, http://dx.doi.org/10.1016/j.agrformet.2016.02.008.
Dahan, O., Tatarsky, B., Enzel, Y., Kulls, C., Seely, M., Benito, G., 2008. Dynamics of flood water infiltration and ground water recharge in hyperarid desert. Ground Water 46, 450–461.
Doane, T.A., Horwáth, W.R., 2003. Spectrophotometric determination of nitrate with a single reagent. Anal. Lett. 36, 2713–2722, http://dx.doi.org/10.1081/AL-120024647.
Dzurella, K.N., Pettygrove, G.S., Fryjoff-Hung, A., Hollander, A., Harter, T., 2015. Potential to assess nitrate leaching vulnerability of irrigated cropland. J. Soil Water Conserv. 70, 63–72, http://dx.doi.org/10.2489/jswc.70.1.63.
Gärdenäs, A.I., Hopmans, J.W., Hanson, B.R., Šimůnek, J., 2005. Two-dimensional modeling of nitrate leaching for various fertigation scenarios under micro-irrigation. Agric. Water Manage. 74, 219–242, http://dx.doi.org/10.1016/j.agwat.2004.11.011.
Goldhamer, D., 2012. Almond in group yield response to water. In: Steduto, P., Hsiao, T.C., Fereres, E., Raes, D. (Eds.), FAO Irrigation and Drainage Paper No.66. Rome, Italy, pp. 246–296.
Goldhamer, D., 2005. Irrigation Management. In: Ferguson, L. (Ed.). University of California Pistachio Production Manual, pp. 103–116.
Green, C.T., Fisher, L.H., Bekins, B.A., 2008. Nitrogen fluxes through unsaturated zones in five agricultural settings across the United States. J. Environ. Qual. 37, 1073–1085, http://dx.doi.org/10.2134/jeq2007.0010.
Hillel, D., 1998. Environmental Soil Physics. Academic Press Publishers, New York.
Ilsemann, J., Goeb, S., Bachmann, J., 2001. How many soil samples are neccessary to obtain a reliable estimate of mean nitrate concentrations in an agricultural field? J. Plant Nutr. Soil Sci. 164, 585, http://dx.doi.org/10.1002/1522-2624(200110)164:5<585:AID-JPLN585>3.0.CO;2-M.
Kass, G.V., 1980. An exploratory technique for investigating large quantities of categorical data. Appl. Stat. 29, 119–127.
Kempers, A.J., Kok, C.J., 1989. Re-examination of the determination of ammonium as the indophenol blue complex using salicylate. Anal. Chim. Acta 221, 147–155, http://dx.doi.org/10.1016/S0003-2670(00)81948-0.
Kendrick, K.J., Graham, R.C., 2004. Pedogenic silica accumulation in chronosequence soils, southern California. Soil Sci. Soc. Am. J. 68, 1295–1303.
King, A.M., Jensen, V.B., Fogg, G., Harter, T., 2012. Addressing Nitrate in California's Water: Technical Report 5 – Remediation of Groundwater. Report [WWW Document] (accessed 9.9.15) http://groundwaternitrate.ucdavis.edu/files/138956.pdf.
Koumanov, K.S., Hopmans, J.W., Schwankl, L.W., 2006. Spatial and temporal distribution of root water uptake of an almond tree under microsprinkler irrigation. Irrig. Sci. 24, 267–278, http://dx.doi.org/10.1007/s00271-005-0027-3.
Kurtzman, D., Shapira, R.H., Bar-Tal, A., Fine, P., Russo, D., 2013. Nitrate fluxes to groundwater under citrus orchards in a Mediterranean climate: observations, calibrated models, simulations and agro-hydrological conclusions. J. Contam. Hydrol. 151, 93–104, http://dx.doi.org/10.1016/j.jconhyd.2013.05.004.
Landon, M.K., Delin, G.N., Komor, S.C., Regan, C.P., 1999. Comparison of the stable-isotopic composition of soil water collected from suction lysimeters, wick samplers, and cores in a sandy unsaturated zone. J. Hydrol. 224, 45–54, http://dx.doi.org/10.1016/S0022-1694(99)00120-1.
Lebese, T., Stassen, P.J.C., Wooldridge, J., 2014. Effects of water and nutrient application frequency on yield: root growth and water usage by Brookfield Gala apple trees. Acta Hortic. 1058, 185–191.
Lopus, S., Santibáñez, M., Beede, R., Duncan, R., Edstrom, J., Niederholzer, F., Trexler, C., Brown, P., 2010. Survey examines the adoption of perceived best management practices for almond nutrition. Calif. Agric. 64, 149–154.
MathWorks, 2012. MATLAB 8.0 and Statistics Toolbox 8.1. The MathWorks, Inc., Natick, Massachusetts, United States.
Maynard, D.G., Kalra, Y.P., Crumbaugh, J.A., 2008. Nitrate and exchangeable ammonium nitrogen. In: Carter, M.R., Gregorich, E.G. (Eds.), Soil Sampling and Methods of Analysis. , 2nd ed. CRC Press, Taylor and Francis Group, Boca Raton, FL, p. 1264, Pages 71–80.
Micke, W., 1996. Almond Production Manual. UC ANR Pub (3364).
Mohannty, B., Kanwar, R., 1994. Spatial variability of residual nitrate-nitrogen under two tillage systems in central Iowa: a composite three-dimensional resistant and exploratory approach. Water Resour. Res. 30, 237–251.
Morgan, K.T., Obreza, T.A., Hanlon, E.A., 2007. Citrus water requirements: linking irrigation scheduling and fertilizer strategies [WWW Document]. Proceeding Florida State Hortic. Soc. (accessed 8.11.15) http://fshs.org/proceedings-o/2007-vol-120/FSHSvol.120/67-73.pdf.
Neilsen, D., Millard, P., Herbert, L.C., Neilsen, G.H., Hogue, E.J., Parchomchuk, P., Zebarth, B.J., 2001. Remobilization and uptake of N by newly planted apple (Malus domestica) trees in response to irrigation method and timing of N application. Tree Physiol. 21, 513–521, http://dx.doi.org/10.1093/treephys/21.8.513.
Onsoy, Y.S., Harter, T., Ginn, T.R., Horwath, W.R., 2005. Spatial variability and transport of nitrate in a deep alluvial vadose zone. Vadose Zone J. 4, 41–54.
Page, R.W., 1986. Geology of the fresh ground-water basin of the Central Valley, California, with texture maps and sections, Professional Paper U.S. Geological Survey, 1401-C. Plate 4.
Pearson, K., 1901. On lines and planes of closest fit to systems of points in space. Philos. Mag. 2, 559–572, http://dx.doi.org/10.1080/14786440109462720.
Perrone, M.P., Cooper, L.N., 1993. When Networks Disagree: Ensemble Methods for Hybrid Neural Networks. In: Chapman-Hall, J.M.R. (Ed.). Neural Networks for Speech and Image Processing, New York.
Phogat, V., Mahadevan, M., Skewes, M., Cox, J.W., 2011. Modelling soil water and salt dynamics under pulsed and continuous surface drip irrigation of almond and implications of system design. Irrig. Sci. 30, 315–333, http://dx.doi.org/10.1007/s00271-011-0284-2.
Phogat, V., Skewes, M.A., Cox, J.W., Sanderson, G., Alam, J., Šimůnek, J., 2014. Seasonal simulation of water, salinity and nitrate dynamics under drip irrigated mandarin (Citrus reticulata) and assessing management options for drainage and nitrate leaching. J. Hydrol. 513, 504–516, http://dx.doi.org/10.1016/j.jhydrol.2014.04.008.
Quiñones, A., Martínez-Alcántara, B., Legaz, F., 2007. Influence of irrigation system and fertilization management on seasonal distribution of N in the soil profile and on N-uptake by citrus trees. Agric. Ecosyst. Environ. 122, 399–409, http://dx.doi.org/10.1016/j.agee.2007.02.004.
Rolston, D.E., Biggar, J.W., Nightingale, H.I., 1991. Temporal persistence of spatial soil-water patterns under trickle irrigation. Irrig. Sci. 12, 181–186, http://dx.doi.org/10.1007/BF00190521.
Russo, D., Laufer, A., Gerstl, Z., Ronen, D., Weisbrod, N., Zentner, E., 2014. On the mechanism of field-scale solute transport: insights from numerical simulations and field observations. Water Resour. Res. 50, 7484–7504, http://dx.doi.org/10.1002/2014WR015514.
Russo, D., Laufer, A., Shapira, R.H., Kurtzman, D., 2013. Assessment of solute fluxes beneath an orchard irrigated with treated sewage water: a numerical study. Water Resour. Res. 49, 657–674, http://dx.doi.org/10.1002/wrcr.20085.
Shapira, H.R., 2012. Nitrate Flux to Groundwater Under Citrus Orchards: Observations, Modeling and Simulating Different Nitrogen Application Rates. MSc. Thesis. The Hebrew University of Jerusalem (in Hebrew).
Siddiqui, M.I., Brown, P., 2013. Pistachio early-season sampling and in-season nitrogen application maximizes productivity. minimizes loss; Protocol for early-season sampling and in-season nitrogen budgeting [WWW Document] (accessed 8.29.15) http://fruitsandnuts.ucdavis.edu/files/165545.pdf.
Silber, A., Xu, G., Levkovitch, I., Soriano, S., Bilu, A., Wallach, R., 2003. High fertigation frequency: the effects on uptake of nutrients, water and plant growth. Plant Soil 253, 467–477, http://dx.doi.org/10.1023/A:1024857814743.
Silva, S.S., Saiful, M., Sanden, B., Laca, E., Brown, P., 2013. Almond early-season sampling and in-season nitrogen ppplication maximizes productivity, minimizes loss—Protocol for early-season sampling and in-season nitrogen budgeting [WWW Document]. URL http://www.almonds.com/sites/default/files/content/attachments/almond_early-season_sampling_and_in-season_nitrogen_application_maximizes_productivity_minimizes_loss.pdf (accessed 8.29.15).
SoilWeb, 2015. SoilWeb—Interactive map of USDA-NCSS soil survey data for locations throughout most of the U.S. [WWW Document]. Calif. Soil Resour. Lab UC Davis UC-ANR Collab. with USDA Nat. Resour. Conserv. Serv. URL (http://casoilresource.lawr.ucdavis.edu/gmap (accessed 8.20.15).
Stenger, R., Priesack, E., Beese, F., 2002. Spatial variation of nitrate-N and related soil properties at the plot-scale. Geoderma 105, 259–275.
Viers, J.H., Liptzin, D., Rosenstock, T.S., Jensen, V.B., Hollander, A.D., McNally, A., King, A.M., Kourakos, G., Lopez, E.M., De La Mora, N., Fryjoff-Hung, A., Dzurella, K.N., Canada, H., Laybourne, S., McKenney, C., Darby, J., Quinn, J.F., Harter, T., 2012. Addressing Nitrate in California's Drinking Water: Technical Report 2—Nitrogen Sources and Loading to Groundwater. Report [WWW Document] (accessed 9.9.15) http://groundwaternitrate.ucdavis.edu/files/138956.pdf.
Vogel, T., Gerke, H.H., Zhang, R., Van Genuchten, M.T., 2000. Modeling flow and transport in a two-dimensional dual-permeability system with spatially variable hydraulic properties. J. Hydrol. 238, 78–89, http://dx.doi.org/10.1016/S0022-1694(00)00327-9.
Walter, M.T., Kim, J.S., Steenhuis, T.S., Parlange, J.Y., Heilig, A., Braddock, R.D., Selker, J.S., Boll, J., 2000. Funneled flow mechanisms in a sloping layered soil: laboratory investigation. Water Resour. Res. 36, 841–849, http://dx.doi.org/10.1029/1999WR900328.
Weissmann, G.S., Zhang, Y., Fogg, G.E., Mount, J.F., 2004. Influence of incised-valley-fill deposits on hydrogeology of a stream-Dominated alluvial fan. In: Bridge, J.S., Hyndman, D. (Eds.), Aquifer Characterization. Special Publications of SEPM, 80. Society for Sedimentary Geology, Tulsa, OK, pp. 15–28.